King Fahd University of Petroleum & Minerals

DEPARTMENT OF MATHEMATICAL SCIENCES

Technical Report Series

TR 208

July 1996

Effects of Relative Permeability History Dependence on Two-Phase Flow in Porous Media

Khaled M. Furati

DHAHRAN 31261 ● SAUDI ARABIA ● www.kfupm.edu.sa/math/ ● E-mail: mathdept@kfupm.edu.sa

Effects of Relative Permeability History Dependence on Two-Phase Flow in Porous Media

Khaled M. Furati

Department of Mathematical Sciences

King Fahd University of Petroleum and Minerals

Dhahran 31261, Saudi Arabia.

Abstract. Hysteresis phenomena in multi-phase flow in porous media has been recognized by many researchers and widely believed to have significant effects on the flow. In an attempt to account for these effects, a theoretical model for history-dependent relative permeabilities is considered. This model is incorporated into two-phase flow and the corresponding flow is predicted. Flow history is observed to have a notable impact on the saturation profile and fluids breakthrough.

Key words: porous media, relative permeability, hysteresis, Riemann problem

1. Introduction

In studies of multiphase flow in porous media, like contaminant and oil reservoir flows, the early practice was to use empirical correlations based on drainage (desaturation of nonwetting phase) conditions alone to characterize flow properties regardless in which direction the saturation change. However, for rocks exhibiting strong wettability preference for a specific phase, experiments have shown that characteristics for imbibition and drainage of the wetting phase are different. The difference is contributed largely to nonwetting phase entrapment and lead to developing flow properties for imbibition as well as drainage flows.

For empirical relations, a typical test for a core sample is performed by first conducting a drainage test until the residual level of the wetting phase saturation is reached. Then an imbibition test starts from this residual saturation until a minimum saturation of the

nonwetting phase is reached. This type of testing establishes bounding drainage-imbibition curves.

Bounding drainage-imbibition curves are useful if we assume that the phases saturation has reached the residual values and the direction of the flow under consideration agrees with the direction of the proceeding flow in a medium. However, in many flows this can not be predicted a priori and the porous medium may not have been subjected to one or more phase saturation extrema. Therefore, appropriate cycles of drainage-imbibition or imbibition-drainage processes should be conducted to obtain relations for possible intermediate flows. These relations are essential for more accurate flow prediction through mathematical models.

Mathematically, this leads to flow functions that are not only functions of current fluid saturation but also of saturation history. One of flow characteristics is the relative permeability. The concept of relative permeability is introduced to describe flow characteristics when more than one immiscible fluid is present in a matrix. To account properly for the history dependence, laboratory tests must be conducted to yield relative permeabilities values that conform with the desired manner a saturation is approached. History dependent relative permeability relations are particularly important for correct predictions in situations involving flow reversals like in enhanced oil recovery and contaminant flow.

There have been many experimental attempts to understand the history dependence of relative permeabilities which in turn lead to other attempts for constructing physical models. Geffen *et al.* [8] and Osoba *et al.* [23] illustrated through several laboratory studies on two-phase systems the history dependence of the relative permeability and the impact of the direction of saturation change on the relative permeability-saturation relations. Naar and Henderson [19] derived a direct relation between the relative permeability characteristics during imbibition and those observed during drainage for two-phase flow in consolidated porous rock. They adapted the model of Wyllie and Gardner [29, 30] to include a trapping mechanism for the nonwetting phase. The extension to three-phase imbibition relative permeability then was made by Naar and Wygal [20]. Naar *et al.* [21] showed experimentally that consol-

idated rocks and unconsolidated porous media exhibit different imbibition flow behavior for two-phase flow. Snell [27] reported the first experimental investigation of history dependence of three-phase relative permeability in unconsolidated sand. Raimondi and Torcaso [25] investigated the distribution of the nonwetting phase resulting from increasing and decreasing the wetting phase saturation in a miscible displacement.

Land [14] developed imbibition relative permeability relations for both two and three-phase systems. In that development, it was assumed that the amount of entrapment at any saturation is a function of the initial nonwetting phase saturation established in the drainage direction and residual saturation after complete imbibition. In a later paper [16], Land verified experimentally these relations for two-phase system. Evrenos and Comer [6] proposed semi-empirical equations for the loci of dynamic hysteresis envelopes and scanning loops spanning the domains of relative permeability for compressible two-phase immiscible displacement. Colonna *et al.* [4] performed experimental work to study the effects of alternate displacements of water and gas on the hydrodynamic characteristics of rock. Based on these experimental results, they proposed a schematic representation of the behavior of the porous medium and the corresponding permeabilities relationship. Killough [13] combined history-dependent relative permeabilities developed by Land [14, 15] with a three-dimensional, three-phase, semi-implicit reservoir simulator.

Jones and Roszelle [12] proposed a graphical technique for determining relative permeabilities for drainage-imbibition flow cycles based on unsteady-state method applied to small linear cores. In a paper by Gladfelter and Gupta [9], a graphical method for predicting the occurrence of an experimentally observed hump, its rate of growth, and saturation within an oil/water bank was developed using the observed hysteresis in fractional flow during a tertiary oil recovery process.

Amaefule and Handy [1] demonstrated experimentally that hysteresis effect is much smaller at low interfacial tension than it is at high interfacial tension. Carlson [3] presented a method for calculating imbibition relative permeability for the nonwetting phase from the drainage

curve, historical maximum nonwetting phase saturation and a minimum of one additional point on some corresponding experimental imbibition curve. In his approach, neither the pore size distribution factor in Land's equation [14] nor the parameter in Killough's [13] approach is necessary. Lenhard [17] developed a predictive model for relative permeabilities in two or three-phase systems subject to arbitrary saturation paths.

For flow predication, there have been many efforts to solve the flow equations but without accounting for the history dependence. Buckley and Leverett [2] constructed the analytical solution for immiscible waterflooding. Pope [24] generalized the fractional flow theory to more complicated floodings and used the method of characteristics to construct the corresponding solutions. The polymer flooding model without hysteresis was analyzed and solved by Isaacson [10] and Johansen and Winther [11].

The first attempt to solve flow equations with history dependence was introduced by Marchesin *et al.* [18]. In that paper, the authors used only a double-valued flux function to model two-phase flow with hysteresis and constructed, graphically, the complete solution of the associated Riemann problem. The author of this paper [7] analyzed and solved the Riemann problem for a polymer flooding model with imbibition-drainage relative permeabilities.

In this paper, we present a general qualitative model for the history dependence of relative permeabilities and the corresponding fractional flow functions. This model is incorporated into the conservation law describing immiscible two-phase flow in porous media and the corresponding Riemann problem solution is constructed. We demonstrate that the flow history might have notable impact on the saturation profile and fluids breakthrough. This implies that more care should be taken when configuring the preinjection conditions and what kind of tests on cores should be conducted to get the desired curves.

The outline of the paper is as follows. In Section 2 we present a physical discussion on the history dependence of relative permeability. In Section 3 we introduce mathematical assumptions and properties of the history dependent functions. In Section 4 and 5 we analyze the flow equations and associated wave families. In Section 6 we construct the global solution

for the Riemann problem. In Section 7 we examine the effects of history on displacement flows. The concluding remarks are given is Section 8.

2. Flow History Dependence Characteristics

The history dependence we consider is based upon the manner in which fluids are distributed in pore spaces initially or during a flow. We start our treatment by introducing some related physical issues.

Relative positions of fluids in individual voids are controlled primarily by the wettability characteristics of the porous medium. In two-phase systems the wetting phase is located as a film over pore walls as well as completely filling some of the smaller pores while the nonwetting phase fills the bigger ones.

When a wetting and nonwetting phase flow together in a porous medium, each follows separate and distinct filamentary paths. Surface tension forces make the wetting phase preferentially fill the smallest of the voids, and the nonwetting phase fill the large spaces between the rock grains, which themselves are covered by a film of the wetting phase. This leads to marked differences in fluids flow behavior based on the direction of saturation change. In particular, this leads to nonwetting phase entrapment.

In view of the above, we should consider different flow characteristics based on whether the wetting or nonwetting phase saturation is increasing. We label a flow *drainage* or *imbibition* according to saturation change of the wetting-phase.

One of the important flow characteristics is the relative permeability. Relative permeability relations should reflect the saturation direction effects for imbibition and drainage flows. As a result, relative permeability should be a function of saturation as well as saturation history that describes the way that saturation is approached.

For a full description of the history dependence of relative permeability, one should consider the following elements.

Irreducible Saturation

Experiments have shown that each maximum saturation for the nonwetting phase results in a different irreducible saturation for the wetting phase. See for example [8] and the references in [14]. Based on these observations, attempts have been made to develop empirical relations. For example, Land [14] used published data to find a relation between the residual nonwetting-phase saturation after imbibition and initial nonwetting phase saturation. From this empirical relation, mathematical expressions were obtained for the trapped and mobile nonwetting-phase saturation.

Hysteresis Magnitude

There have been many attempts to describe the magnitude of hysteresis in relative permeability relations. Some laboratory investigations have shown that the wetting-phase imbibition and drainage relative permeabilities show little deviation from each other [9, 16], while considerable differences has been observed for the nonwetting phase relative permeabilities. On the other hand, other investigations indicated that both wetting and nonwetting phase relative permeabilities may exhibit hysteresis and the greater the trapped saturation, the greater the imbibition wetting-phase relative permeability. In many experiments it has been observed that for the nonwetting phase at a given saturation, imbibition relative permeability is smaller than the drainage one while the opposite was observed for the wetting phase relative permeabilities [1, 8, 16, 21, 23, 25]. The contrary behavior have been reported for unconsolidated porous media [21]. In yet other experiments, effects different from the above have been noticed [4, 9].

Reversibility

Many experiments have shown that relative permeability curves reach stability after a cycle of flow reversal. In particular, when reversing the flow direction from drainage to imbibition, the imbibition curve is reversible. In other wards, once a nonwetting phase saturation has been established and the flow behavior has been determined in imbibition direction, this flow behavior is reversible and reproducible, provided the previous maximum nonwetting phase saturation is not exceeded [8, 16, 25, 26]. A justification for this behavior is that, the trapped fluids are distributed within a range of pore sizes in such a way that if the direction of the saturation change is reversed from imbibition to drainage, the trapped fluids are released in the reverse order of entrapment. In this paper, we assume that relative permeability curves for wetting and nonwetting phase exhibit a more or less reversible nature.

Porous Medium History

The initial saturation history of a porous medium depends on the extreme values of saturation reached in that medium. For example, a typical oil reservoir may initially contain connate water and oil as a result of oil invasion of pores. After a period of primary production, water (wetting) often enters the reservoir either from the surrounding aquifers or surface injections and leads to an imbibition flow. In this scenario the reservoir can be assumed to have a drainage history followed by an imbibition. Accordingly, the current relative permeability values lie on an imbibition curve determined by the maximum saturation reached during the drainage process. On the other hand, if the reservoir is depleted by decreasing the oil (wetting) saturation and increasing the gas saturation, as in a dissolved-gas drive, the drainage relative permeability curves corresponding to the maximum saturation occurred during oil imbibition apply. Another example, in contaminant flow, when a porous medium has been through a sequence of events of water drainage, rainfall, contaminant leakage, etc. [17].

3. Mathematical Description for Saturation Functions

In this section we describe mathematically the different saturation functions and their history dependence based on the physical characteristics presented above. We discuss the mathematical assumptions and properties of relative permeabilities and their implications on fractional flows. Saturation functions vary according to the following types of flow.

3.1. Primary Flow

Consider the case when pores are completely filled with a nonwetting (nw) phase. We call the displacement of this fluid by a wetting (w) phase *primary imbibition*. Similarly, *primary drainage* is the flow in which a nonwetting phase displaces the wetting phase filling completely the pores.

Let S denote the wetting phase saturation. Let S_{rw} and S_{rnw} be the irreducible saturation for the wetting and nonwetting phase, respectively. For $j = w$ or nw, let $K^i_{rj}(S)$ and $K^d_{rj}(S)$ denote the relative permeability for primary imbibition and drainage, respectively. Then, $K^i_{rw}(S)$ and $K^d_{rw}(S)$ are increasing functions of S while $K^i_{rnw}(S)$ and $K^d_{rnw}(S)$ are decreasing functions of S.

We assume that the primary relative permeabilities are C^2 functions and convex (positive second derivative) for $S_{rw} < S < 1 - S_{rnw}$. Typical primary relative permeability curves are shown in Figure 1. The wetting fractional flow function is defined by

$$F^p(S) = \frac{K^p_{rw}(S)}{K^p_t(S)}, \qquad K^p_t(S) = K^p_{rw}(S) + \mu\, K^p_{rnw}(S), \qquad p = i, d. \tag{1}$$

Where, $\mu = \mu_{nw}/\mu_w$ is the viscosity ratio. Note that F^p is a C^2 increasing function for $S_{rw} < S < 1 - S_{rnw}$. Typically, curves of F^p have inflection points. To guarantee this we assume that

$$\frac{dK^p_t}{dS}(S_{rw}) \le 0, \qquad \frac{dK^p_t}{dS}(1 - S_{rnw}) \ge 0. \tag{2}$$

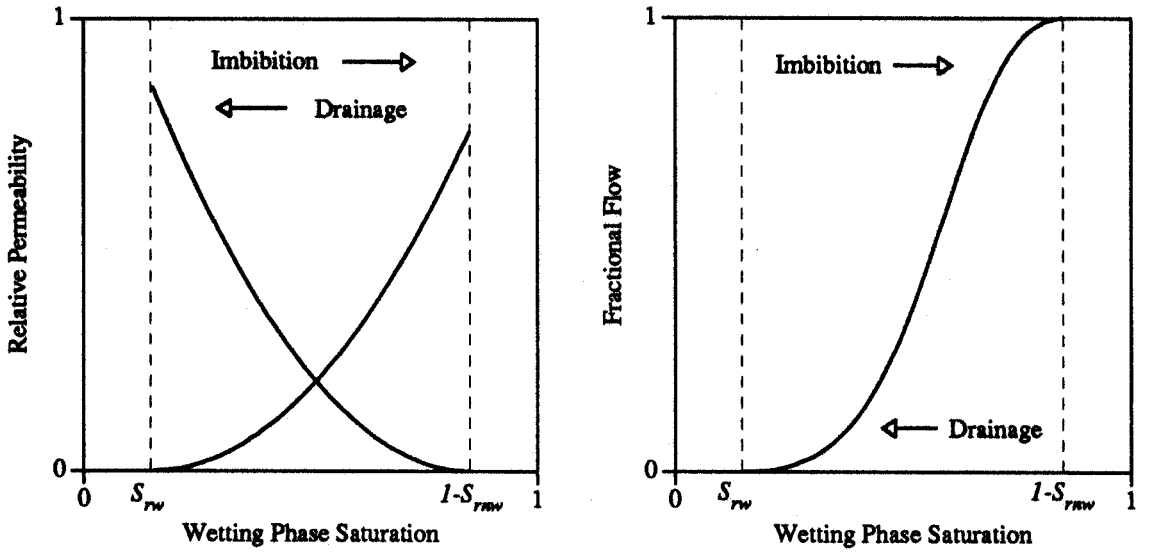

Figure 1. Primary flow curves.

According to (38) and (40) in the Appendix, condition (2) is a sufficient condition for the primary fractional flow function, F^p, to be convex in a neighborhood of $S = S_{rw}$ and concave in a neighborhood of $S = 1 - S_{rnw}$. This implies the existence of an inflection point of F^p. However, for most applications, experimental data indicates that the fractional flow function has at most one inflection point. Therefore, we assume that S_{inf} is the only point of inflection, and consequently, for $p = i$ and $p = d$, F^p is convex in (S_{rw}, S_{inf}) and concave in $(S_{inf}, 1 - S_{rnw})$ as shown in Figure 1.

3.2. Secondary Flows

If a flow reversal occurs during a primary flow, we call the flow a *secondary flow.* This includes the secondary drainage of a primary imbibition (id) and secondary imbibition of a primary drainage (di). We denote the critical saturation at which the flow reversal occurs by S_h, where $h = id, di$, indicates the relevant flow cycle for the secondary flow.

For secondary flows, we denote the relative permeability function of the j-phase, $j = w, nw$, by K^h_{rj}. If necessary, we use the superscripts u and l to indicate whether at any saturation the relative permeability value is greater than or less than the one for the primary flow, respectively. In other wards, for any saturation S, the relative permeabilities are related as

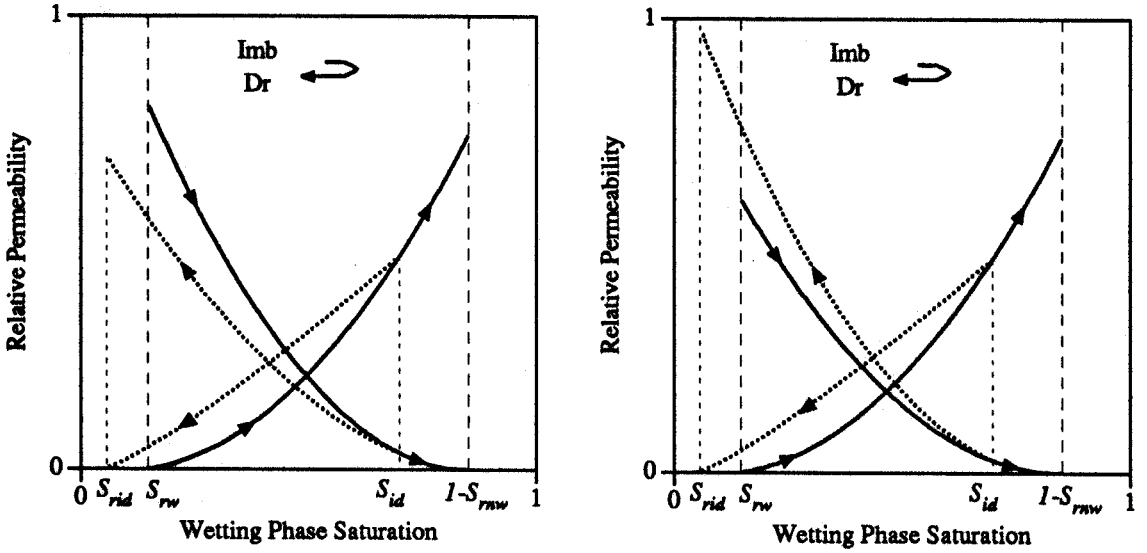

Figure 2. Relative permeability curves for *id* flow with $K^{id,u}$.

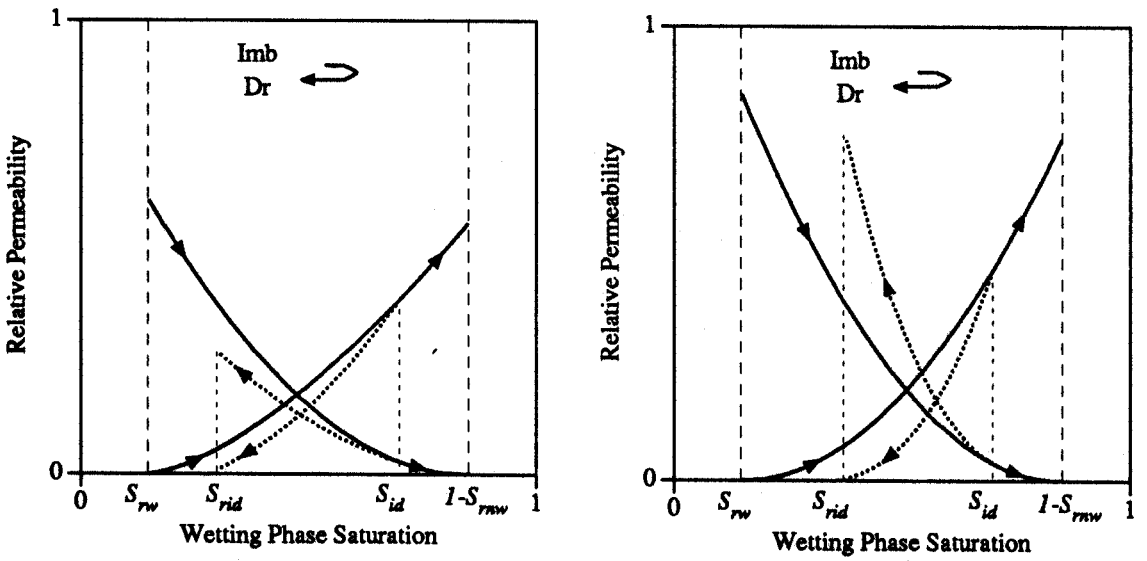

Figure 3. Relative permeability curves for *id* flow with $K^{id,l}$.

follows:

$$K_{rj}^{id,l}(S, S_{id}) \leq K_{rj}^{i}(S) \leq K_{rj}^{id,u}(S, S_{id}), \qquad K_{rj}^{di,l}(S, S_{di}) \leq K_{rj}^{i}(S) \leq K_{rj}^{di,u}(S, S_{di}). \tag{3}$$

Typical curves are shown in Figures 2– 5. Although, some of these curves may not be observed experimentally, we consider all the possibilities of disjoint curves for the purpose of completeness.

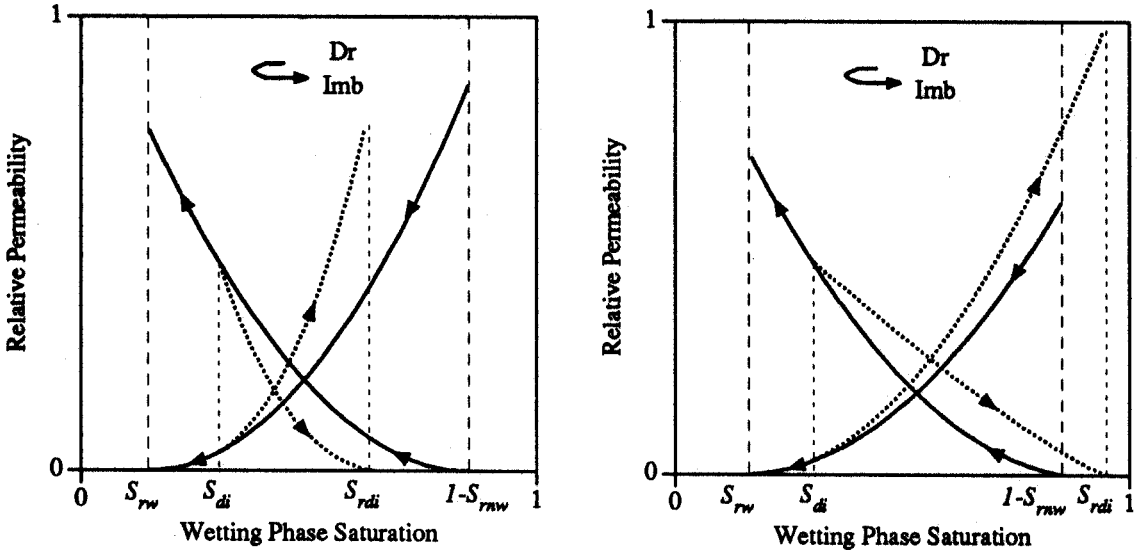

Figure 4. Relative permeability curves for *di* flow with $K^{di,u}$.

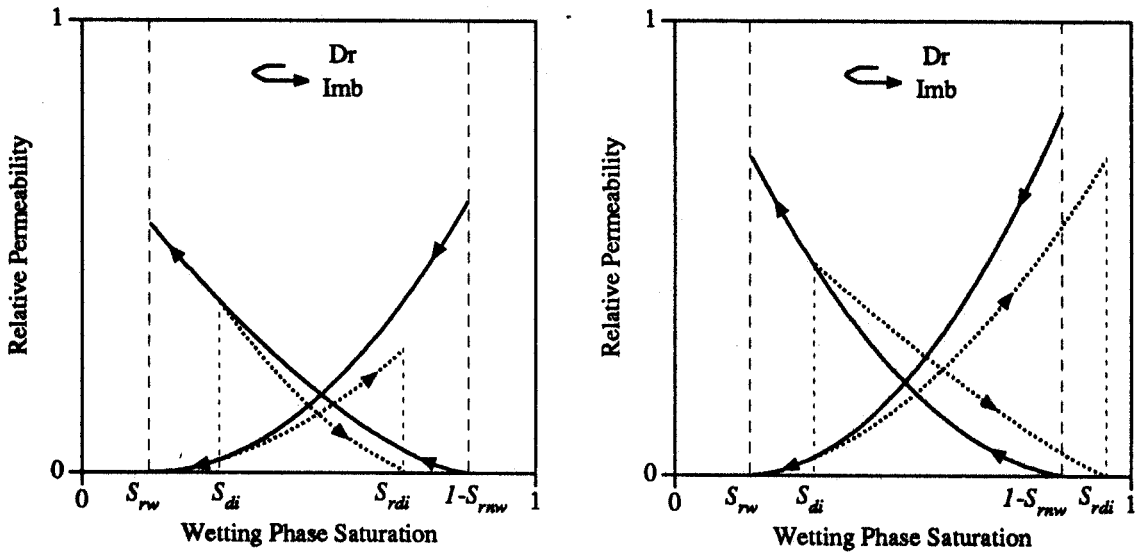

Figure 5. Relative permeability curves for *di* flow with $K^{di,l}$.

The irreducible saturation of a secondary flow is a function of the critical saturation S_h. We define the irreducible saturations by

$$S_{rid}(S_{id}) = \max\{S : K^{id}_{rw}(S, S_{id}) = 0\}, \tag{4}$$

and

$$S_{rdi}(S_{di}) = \min\{S : K^{di}_{rnw}(S, S_{di}) = 0\}. \tag{5}$$

Accordingly, the domain of secondary relative permeability functions consists of the saturation values that lie between S_h and S_{rh}.

We assume that K^h_{rw} is an increasing function of the wetting phase saturation S while K^h_{rnw} is decreasing. Moreover, we assume that the transition from primary to secondary flow is continuous, i.e.,

$$K^h_{rj}(S_h, S_h) = K_{rj}(S_h), \tag{6}$$

and that all $K^h_{rj}(S, .)$ functions are C^1 in their domain. Moreover, for a fixed S_h, $S_{rw} \leq S_h \leq 1 - S_{rnw}$, we assume that $K^h_{rj}(., S_h)$ is C^2 and convex in its domain. We also assume that the secondary relative permeability curves are disjoint for distinct values of S_h. Or,

$$\partial_{S_h} K^{id,u}_{rw} > 0, \qquad \partial_{S_h} K^{id,l}_{rw} < 0, \qquad \partial_{S_h} K^{di,u}_{rw} < 0, \qquad \partial_{S_h} K^{di,l}_{rw} > 0. \tag{7}$$

The condition (7) and definition of left and right derivatives, ∂^-_S and ∂^+_S, respectively, as in (41) of the Appendix also imply that

$$\partial^-_S K^{id,u}_{rw}(S_h, S_h) \leq \partial_S K^i_{rw}(S_h) \leq \partial^-_S K^{id,l}_{rw}(S_h, S_h), \tag{8}$$

and

$$\partial^+_S K^{di,l}_{rw}(S_h, S_h) \leq \partial_S K^i_{rw}(S_h) \leq \partial^+_S K^{di,u}_{rw}(S_h, S_h). \tag{9}$$

The analog holds for the nonwetting phase relative permeabilities.

We define the secondary fractional flow function $F^h(S, S_h)$ for the wetting phase by

$$F^h(S, S_h) = \frac{K^h_{rw}(S, S_h)}{K^h_{rw}(S, S_h) + \mu\, K^h_{rnw}(S, S_h)}, \qquad h = id, di. \tag{10}$$

Note that the transition from primary to secondary flow is continuous and that $F^{id}(S_{rid}, S_{id}) = 0$ while $F^{di}(S_{rdi}, S_{di}) = 1$. Moreover, note that $F^h(., S_h)$ is C^2 while $F^h(S, .)$ is C^1 in their domains. From equation (29) in the Appendix, for each S_h, F^h is an increasing function of the wetting saturation S.

Note that given S_{id}, we have

$$F^i = \frac{K^i_{rw}}{K^i_{rw} + \mu\, K^i_{rnw}} \leq \frac{K^{id,u}_{rw}}{K^{id,u}_{rw} + \mu\, K^{id,l}_{rnw}} \tag{11}$$

Table I. Secondary fractional flow curves behavior.

K^h_{rw}	K^h_{rnw}	$\partial_{S_h} K^h_{rw}$	$\partial_{S_h} K^h_{rw}$		$F^h - F^p$	$\partial_{S_h} F^h$	F^h
$p = i, h = id$							
$K^{id,u}_{rw}$	$K^{id,l}_{rnw}$	> 0	< 0	implies	> 0	> 0	$F^{id,u}$
$K^{id,u}_{rw}$	$K^{id,u}_{rnw}$	> 0	> 0	assume	> 0	> 0	$F^{id,u}$
$K^{id,l}_{rw}$	$K^{id,u}_{rnw}$	< 0	> 0	implies	< 0	< 0	$F^{id,l}$
$K^{id,l}_{rw}$	$K^{id,l}_{rnw}$	< 0	< 0	assume	< 0	< 0	$F^{id,l}$
$p = d, h = di$							
$K^{di,u}_{rw}$	$K^{di,l}_{rnw}$	< 0	> 0	implies	> 0	< 0	$F^{di,u}$
$K^{di,u}_{rw}$	$K^{di,u}_{rnw}$	< 0	< 0	assume	> 0	< 0	$F^{di,u}$
$K^{di,l}_{rw}$	$K^{di,u}_{rnw}$	> 0	< 0	implies	< 0	> 0	$F^{di,l}$
$K^{di,l}_{rw}$	$K^{di,l}_{rnw}$	> 0	> 0	assume	< 0	> 0	$F^{di,l}$

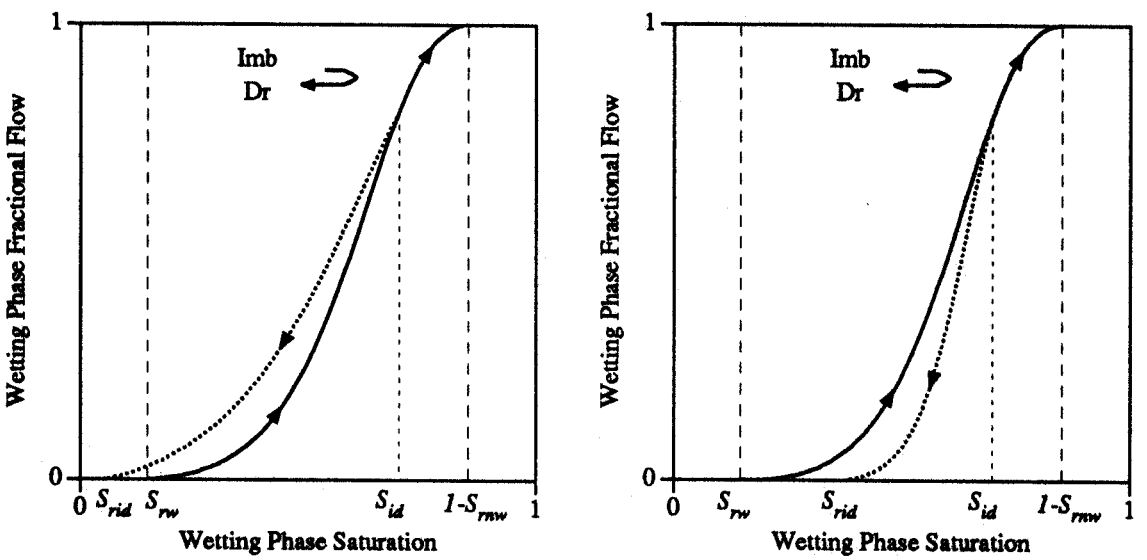

Figure 6. Fractional flow curves for *id* flow.

for $S_{rid} < S < S_{id}$. Moreover, from (30) in the appendix, the ∂_{S_h} derivative of the right hand side function is positive. This implies that the corresponding secondary curves lie above the primary curve and are disjoint. We denote such curves by $F^{id,u}$. This is not true in general for $K^{id,u}_{rw}/[K^{id,u}_{rw} + \mu\, K^{id,u}_{rnw}]$. However, for this case we assume that the secondary curves are of $F^{id,u}$ type. Table I summarizes all the possible cases we consider for F^h, $h = id, di$. The curves of these cases are shown in Figures 6 and 7.

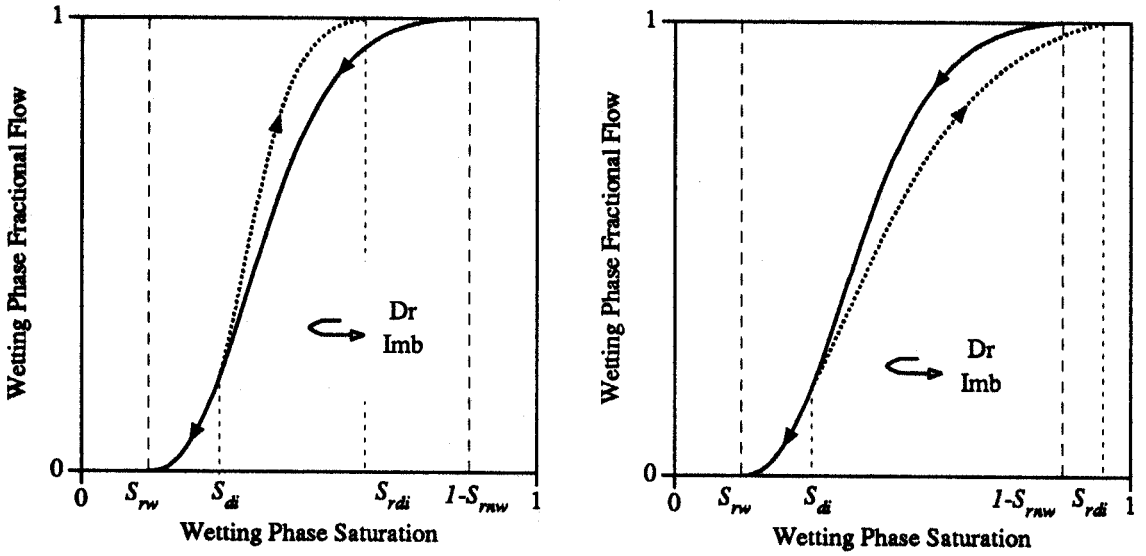

Figure 7. Fractional flow curves for *di* flow.

Note that the curves slope at the critical saturation satisfies

$$\partial_S^- F^{id,u}(S_h, S_h) \leq \partial_S F^i(S_h) \leq \partial_S^- F^{id,l}(S_h, S_h), \tag{12}$$

and

$$\partial_S^+ F^{di,l}(S_h, S_h) \leq \partial_S F^i(S_h) \leq \partial_S^+ F^{di,u}(S_h, S_h). \tag{13}$$

We assume that the curves of F^{id} are convex in some neighborhood of S_{rid} and the curves of F^{di} are concave in a neighborhood of S_{rdi}. By equations (34) and (36) of the Appendix, sufficient conditions for this behavior are

$$\partial_S K_{rw}^{id}(S_{rid}, S_{id}) + \mu\, \partial_S K_{rnw}^{id}(S_{rid}, S_{id}) \leq 0, \tag{14}$$

and

$$\partial_S K_{rw}^{di}(S_{rid}, S_{di}) + \mu\, \partial_S K_{rnw}^{di}(S_{rdi}, S_{di}) \geq 0. \tag{15}$$

Unlike the primary fractional flow function, assumptions on $K_{rw}^h(S, S_h)$ and $K_{rnw}^h(S, S_h)$ guarantee neither existence nor uniqueness of inflection points for secondary fractional flow functions. We assume that any secondary fractional flow function has at most one inflection point.

4. Flow Equations

Simultaneous flow of two immiscible phases is described by the basic equations: volume balance, Darcy's law and conservation of mass. We assume that the porous medium is homogeneous, so that the porosity and total permeability of the rock are constant. For the phases, we assume incompressibility and constant viscosity. Moreover, we assume that diffusive forces, such as capillary pressure, are negligible and the flow is horizontal so there is no gravity effect. We also assume that the flow is one-dimensional with constant total velocity.

Under these assumptions the basic equations reduces to the dimensionless single conservation law, known in literature as Buckley-Leverett equation [2],

$$\partial_t S + \partial_x F = 0, \tag{16}$$

where S and F are the saturation and fractional flow function, respectively, for the wetting phase. For more details on the derivation of (16) and physical assumptions see [24].

The fractional flow function F is history dependent and determined by the type of the flow. In other words,

$$F = \begin{cases} F^p(S) & \text{for primary flow,} \\ F^h(S, S_h) & \text{for secondary flow.} \end{cases} \tag{17}$$

The conservation law (16) requires initial data for S and S_h at each point in space. We consider the Riemann initial condition:

$$(S, S_h)(x, 0) = \begin{cases} (S^L, S_h^L) & x \leq 0, \\ (S^R, S_h^R) & x > 0, \end{cases} \tag{18}$$

where for the primary flow the initial condition (18) reduces to values for S only since $S_h = S$. The solution of (16) and (18) describes the saturation distribution and history at each point of space and time.

If the flow is secondary, $F = F^h(S, S_h)$, then the conservation law (16) can be closed by adding the constraint $\partial_t S_h = 0$ for the reversibility assumption. The two equations can be

written in the quasilinear form

$$\partial_t \begin{bmatrix} S \\ S_h \end{bmatrix} + A\,\partial_x \begin{bmatrix} s \\ S_h \end{bmatrix} = 0, \qquad A = \begin{bmatrix} \partial_S F^h & \partial_{S_h} F^h \\ 0 & 0 \end{bmatrix}. \tag{19}$$

The characteristic speeds and their corresponding eigenvectors are

$$\lambda_h = \partial_S F^h, \quad r_s = \begin{bmatrix} 1 \\ 0 \end{bmatrix}, \qquad \lambda_{st} = 0, \quad r_{st} = \begin{bmatrix} \partial_{S_h} F^h \\ -\partial_S F^h \end{bmatrix}. \tag{20}$$

Note that the characteristic speed λ_h is the slope of F^h which is nonnegative while the other characteristic speed λ_{st} is identically zero. This implies that all wave families are either stationary or traveling to the right.

When the flow is primary, equation (19) reduces to the single equation

$$\partial_t S + \lambda_p \partial_x S = 0, \tag{21}$$

where $\lambda_p = (F^p)'$ is the characteristic speed and equals to the slope of F^p.

For the transitional states (S_h, S_h), we define the characteristic speeds by:

$$\lambda_p(S_h) = \partial_S F(S_h), \qquad \lambda_h(S_h, S_h) = \partial_S^\alpha F^h(S_h, S_h), \tag{22}$$

where, ∂_S^α is the appropriate right or left derivative. The type of the flow (secondary or primary) determines which velocity is to be used in determining Riemann problem solutions.

5. Waves Families

Solutions of the Riemann problem for conservation laws consist of elementary waves. Given left and right states, then at any time the saturation profile consists of self-sharpening fronts (*shocks*), expansion waves (*rarefactions*) and contact discontinuities.

The corresponding waves to the zero characteristic speed λ_{st} are stationary contact discontinuities since the field is linearly degenerate. On the other hand, due to the inflection points of F^p and F^h, the p-family and h-family are not typically genuinely nonlinear since

$$\nabla \lambda_h \cdot r_s = \partial_{SS} F^h, \qquad \nabla = (\partial_S, \partial_{S_h}). \tag{23}$$

Thus both families consist of rarefactions and shocks.

As we know, any discontinuity solution of speed σ must satisfy the Rankine-Hugoniot condition. For the secondary flow, the Rankine-Hugoniot condition takes the form

$$\begin{bmatrix} (F^h)^R - (F^h)^L \\ 0 \end{bmatrix} = \begin{bmatrix} S^R - S^L \\ S_h^R - S_h^L \end{bmatrix} \sigma. \tag{24}$$

The condition (24) is satisfied by two kinds of discontinuities. The first one is a shock that travels with speed

$$\sigma = \frac{(F^h)^R - (F^h)^L}{S^R - S^L} \tag{25}$$

and across which the history parameter S_h is constant. The second discontinuity is a stationary one across which the fractional flow is continuous. This saturation discontinuity is associated with the characteristic speed λ_{st}.

For the primary flow, the Rankine-Hugoniot condition reduces to

$$(F^p)^R - (F^p)^L = \sigma\,(S^R - S^L). \tag{26}$$

This discontinuity is a shock that travels with speed σ.

To distinguish the physically meaningful shocks, we need to impose an entropy condition. For our purpose, a shock is considered admissible if it satisfies the Oleinik condition [22] for scalar equations. For a fractional flow function $F = F^p$ or F^h, Oleinik condition requires that

$$\frac{F^R - F(S, S_h)}{S^R - S} \leq \sigma = \frac{F^R - F^L}{S^R - S^L} \tag{27}$$

for all S between S^L and S^R. In other words, the chord from (S^R, F^R) to (S^L, F^L) must lie above the chord from (S^R, F^R) to $(S, F(S, S_h))$ for any S in between.

In a rarefaction, the saturation distribution is continuous in space and the velocity of a given saturation is equal to the characteristic speed λ_p or λ_h. For this profile, the characteristic speeds should be monotonically increasing from left to right.

The monotonicity and Oleinik condition are equivalent to the construction of the concave hull when $S^L > S^R$ and convex hull when $S^L < S^R$ for the fractional flow curves as shown

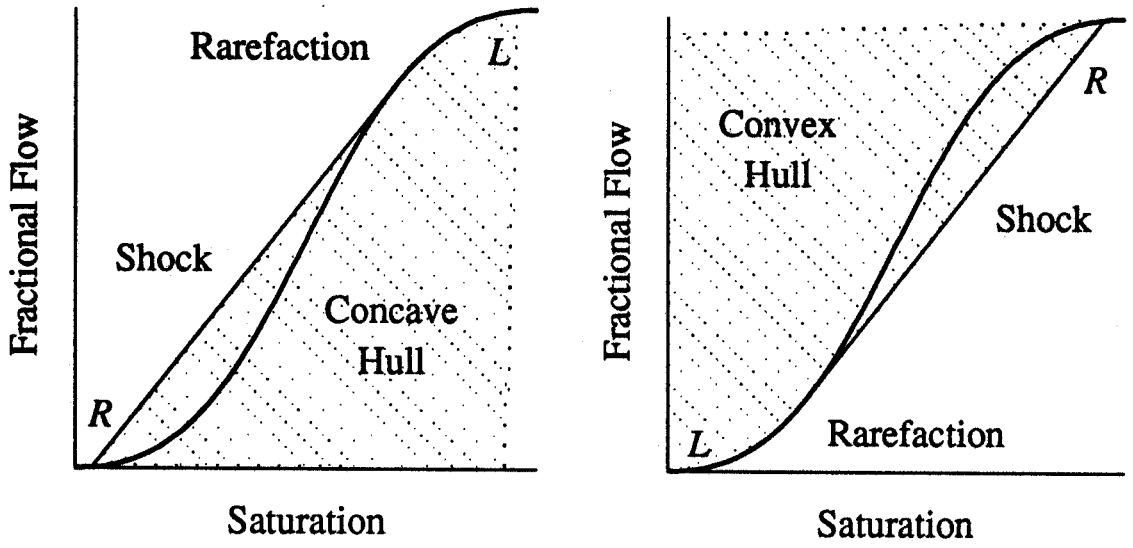

Figure 8. Concave and convex hulls.

in Figure 8. A straight line segment represents a shock and a curve segment represents a rarefaction. The shock speed is equal to the slope of the straight line. The stationary contact discontinuity corresponds to a horizontal line connecting the left and right states since the fractional flow is constant.

In petroleum engineering literature, the above solutions are usually explained in terms of Welge tangents [5, 28]. Welge tangents are equivalent to Oleinik chords for such problems.

6. Riemann Problem Solution

The global solution to the Riemann problem can be constructed graphically using the wave families mentioned above. Uniqueness of solutions can be easily verified by imposing the compatibility condition, i.e., the initial speed of each wave is greater than or equal to the final speed of the preceding wave.

Note that for any given left and right state, the horizontal line through the left state intersects the secondary fractional flow curve associated with S_h^R provided that the fractional flow value for S_h^R is greater (less) than the value of the left state for *id* (*di*) flows. Otherwise, the horizontal line intersects only with the primary curve at some saturation $S = S^P$. Please,

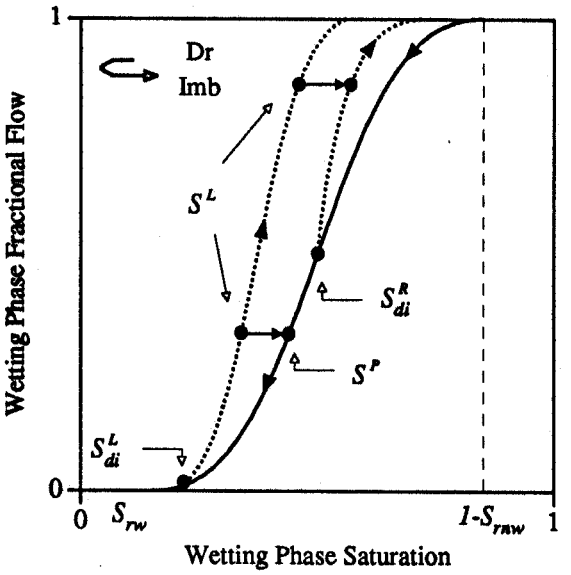

Figure 9. Stationary wave solution.

see Figure 9. This horizontal line represents a stationary contact discontinuity. Since this discontinuity is stationary and all other wave solutions travel to the right, we can reduce the Riemann problem to cases for which either the left and right history are the same ($S^L_h = S^R_h$) or the initial left flow is primary ($S^L = S^L_h$).

The stationary contact discontinuity is an outcome of the reversibility assumption on the flow ($\partial_t S_h = 0$). Physically, this discontinuity acts as an adjustment for the saturation to keep the same rate of flow for two adjacent parts of the porous medium with different histories.

In view of the above observation and without lose of generality, we only consider the following two cases for the initial left and right states.

(a) Equal Left and Right History

In this case, both left and right state fractional flow values are given by the secondary curve associated with $S^R_h = S^L_h$. The solution is determined by the concave hull if $S^R < S^L$ or by the convex hull if $S^R > S^L$. Thus, we have an h-wave connecting the left and right state across which S_h is constant and is equal to S^R_h.

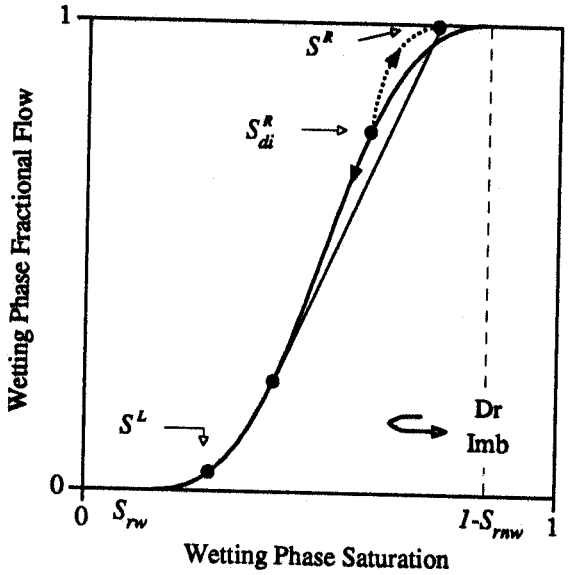

Figure 10. Solution for initial primary left *di* flow.

(b) Primary Initial Left Flow

In this case we have $S^L = S^L_{di} \leq S^R_{di} \leq S^R$ for *di* flow and $S^R \leq S^R_{id} \leq S^L = S^L_{id}$ for *id* flow. For a *di* flow, note that the left state (S^L, S^L) can be connected to the critical state (S^R_{di}, S^R_{di}) by a unique *p*-wave determined by the convex hull of the primary curve joining the two states. On the other hand, the critical state (S^R_{di}, S^R_{di}) can be connected to the right state (S^R, S^R_{di}) by a unique *h*-wave determined by the convex hull of the secondary curve. If the union of the two convex hulls is also convex then the two waves are compatible. Otherwise, the solution is given by the convex hull of the union of the two convex hulls as shown in Figure 10. The solution for an *id* flow is obtained using the same construction but for concave hulls instead.

7. History Effects on Displacement Processes

In this section we evaluate the impact of flow history on two-phase systems. For this purpose, we investigate displacement processes in which a fluid is injected into a porous medium. We denote the preinjection fluid composition in a porous medium by (S^I, S^I_h) and the injected

fluid saturation by S^J. Initial saturation history S_h^I depends on the sequence of events the porous medium exposed to or went through. In view of this, we consider the following scenarios for preinjection flow in a porous medium.

(a) Primary Preinjection Flow

In this flow the porous medium is assumed to undergo a primary flow through either primary drainage or imbibition. This corresponds to the initial condition with $S^I = S_h^I$ and thus the flow values are extracted from the primary curve.

(b) Secondary Preinjection Flow

If, however, the porous medium under consideration is assumed to be exposed to an event of flow reversal at some saturation S_h^I, then the preinjection fluid characteristics are determined by the secondary fractional flow curve associated with S_h^I.

Based on these two preinjection flows, there are three consequent displacement flows that can take place.

(a) Primary Flow Displacement

If the preinjection flow in a porous medium is primary and the injected fluid saturation value, S^J, agrees with the monotone direction of the saturation change for that flow, then the entire displacement flow is primary. This takes place when $S^J > S^I$ for *id* flow as well as when $S^J < S^I$ for *di* flow. In both cases we have $S^J = S_h^J$. In such a displacement, saturation history is irrelevant.

(b) Secondary Flow Displacement

On the other hand, if the preinjection flow in a porous medium is secondary and the injected saturation value, S^J, agrees with the monotone direction of the saturation change for that flow then the displacement process is entirely a secondary flow. This situation arises if either

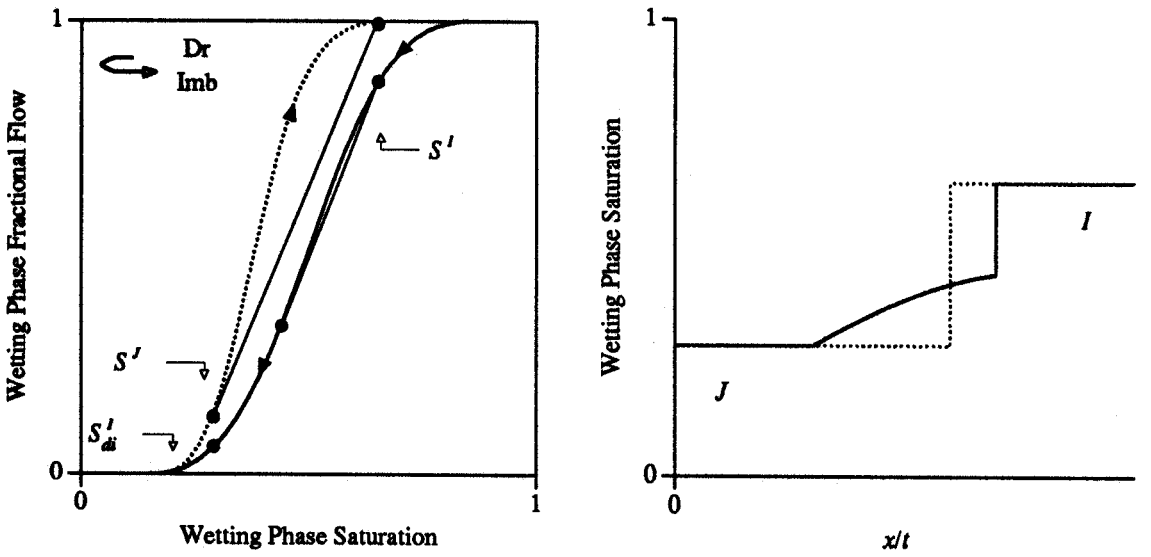

Figure 11. History Effects on *di* flow displacements.

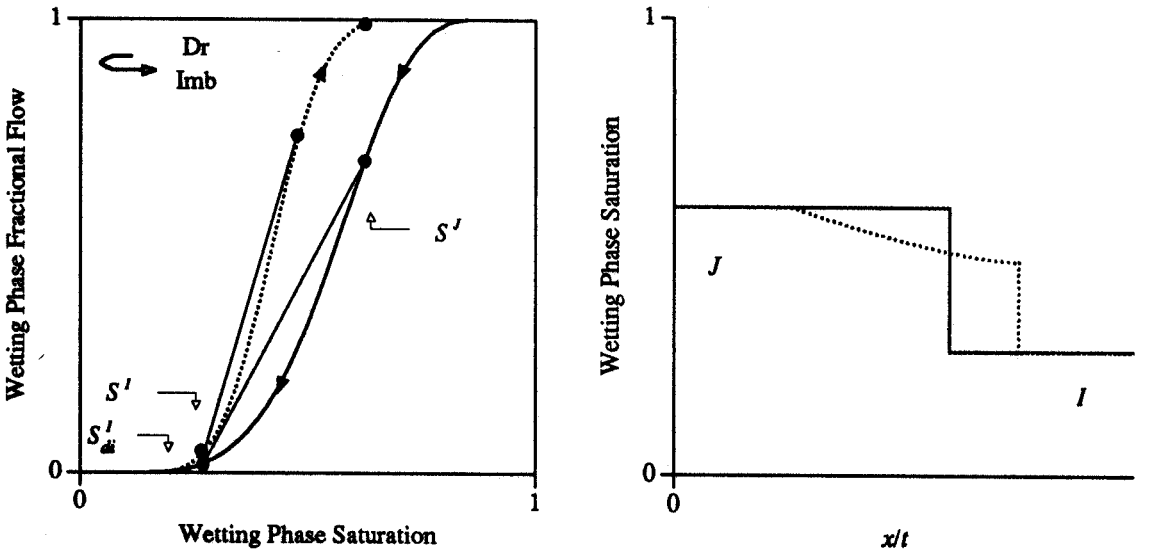

Figure 12. History Effects on *di* flow displacements.

$S^J > S^I_h$ for *di* flow or $S^J < S^I_h$ for *id* flow. As a result, the saturation profile is determined by the hulls of the secondary curve associated with S^I_h. Using the secondary curve rather than primary curve in this case leads to different hulls and thus a different saturation profile. In Figures 11 and 12 we present examples of displacements in a *di* flow. These examples demonstrate history effects on the saturation profile and compare the flow with (solid curves) and without (dashed curve) accounting for flow history. We notice that, flow history not only effects fronts and rarefactions speed, but also interchanges a front combined with an

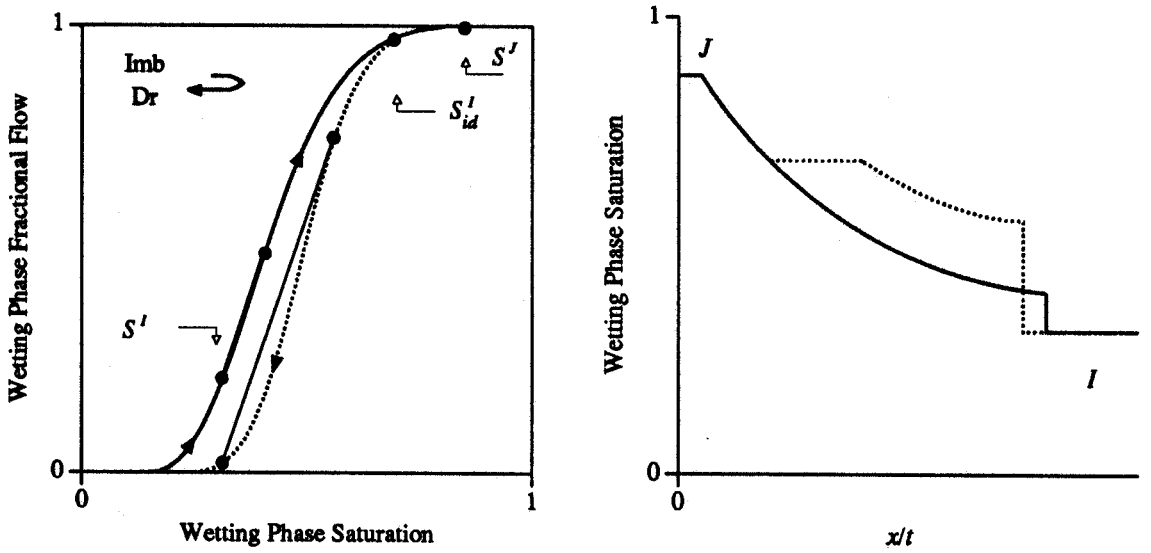

Figure 13. History Effects on *id* flow displacement.

expansion wave by a single front and vice versa. Similar effects exist for the other types of flow.

(c) Secondary-Primary Flow Displacement

Finally, consider the case when the injected fluid saturation value, S^J, is less than S^I_{di} or greater than S^I_{id}. Then, at each position in the porous medium, the displacement process starts as a secondary flow followed by a primary one. The saturation profile is determined by constructing the appropriate hull for both the primary and secondary curves. For such displacement, taking into account the history effects may result in saturation profiles with reduced or increased number of fronts or expansions as well as different breakthrough times. In Figure 13 we present an example for an *id* flow.

8. Concluding Remarks

– Saturation history of a porous medium has a variety of implications on the flow, even with reversibility assumption. Including history dependence may result in flows with different number of fronts and expansions as well as different traveling speeds of waves.

- To reach the right prediction for a two-phase flow in a porous medium, it is imperative that laboratory tests be conducted with a saturation history simulating that of the medium being under consideration.
- Displacement processes can be made more efficient by modifying the preinjection history of the porous medium to get the preferred breakthrough time or rate of advance of a certain composition. This has important economic implications in enhanced oil recovery, contaminant cleanup and similar processes in which the porous media is exposed to successive cycles of productions or flows.
- The observed history effects under the reversibility assumption suggest that more investigation is to be done for cyclic history dependence.

Acknowledgements

The author is grateful for the financial support provided by King Fahd University of Petroleum and Minerals.

Appendix

Mathematical Expressions

For secondary fractional flow functions,

$$F^h(S, S_h) = \frac{K^h_{rw}(S, S_h)}{K^h_{rw}(S, S_h) + \mu\, K^h_{rnw}(S, S_h)}, \tag{28}$$

the first derivatives are

$$\partial_S F^h = \frac{\mu}{(K^h_t)^2}\left[K^h_{rnw}\,\partial_S K^h_{rw} - K^h_{rw}\,\partial_S K^h_{rnw}\right] \geq 0 \tag{29}$$

and

$$\partial_{S_h} F^h = \frac{\mu}{(K_t^h)^2}\left[K_{rnw}^h\,\partial_{S_h} K_{rw}^h - K_{rw}^h\,\partial_{S_h} K_{rnw}^h\right], \tag{30}$$

where,

$$K_t^h = K_{rw}^h + \mu\, K_{rnw}^h \tag{31}$$

The ∂_{SS} derivative is

$$\partial_{SS} F^h = \frac{\mu}{(K_t^h)^3} \tag{32}$$
$$\left\{K_t^h\left[K_{rnw}^h\,\partial_{SS} K_{rw}^h - K_{rw}^h\,\partial_{SS} K_{rnw}^h\right] - 2\,\partial_S K_t^h\left[K_{rnw}^h\,\partial_S K_{rw}^h - K_{rw}^h\,\partial_S K_{rnw}^h\right]\right\}.$$

Note that similar expressions hold for F^p with ∂_S replaced by $' = d/dS$.

When $(S, S_h) = (S_{rid}, S_{id})$ the derivatives for the *id* fractional flow function reduces to

$$\partial_S F^{id} = \frac{1}{\mu}\frac{\partial_S K_{rw}^{id}}{K_{rnw}^{id}} \geq 0 \tag{33}$$

and

$$\partial_{SS} F^{id} = \frac{1}{\mu^2 (K_{rnw}^{id})^2}\left\{\mu\, K_{rnw}^{id}\,\partial_{SS} K_{rw}^{id} - 2\,\partial_S K_t^{id}\,\partial_S K_{rw}^{id}\right\}. \tag{34}$$

The derivatives for the *di* fractional flow function at $(S, S_h) = (S_{rdi}, S_{di})$ are

$$\partial_S F^{di} = -\mu\frac{\partial_S K_{rnw}^{di}}{K_{rw}^{di}} \geq 0 \tag{35}$$

and

$$\partial_{SS} F^{di} = \frac{-\mu}{(K_{rw}^{di})^2}\left\{K_{rw}^{di}\,\partial_{SS} K_{rnw}^{di} - 2\,\partial_S K_t^{di}\,\partial_S K_{rnw}^{di}\right\} \tag{36}$$

For primary fractional flow functions, when $S = S_{rw}$ we get

$$(F^p)' = \frac{1}{\mu}\frac{(K_{rw}^p)'}{K_{rnw}^p} \geq 0 \tag{37}$$

and

$$(F^p)'' = \frac{1}{\mu^2 (K_{rnw}^p)^2}\left\{\mu\, K_{rnw}^p (K_{rw}^p)'' - 2\,(K_t^p)'(K_{rw}^p)'\right\} \tag{38}$$

However, for $S = 1 - S_{rnw}$, we have

$$(F^p)' = -\mu \frac{(K^p_{rnw})'}{K^p_{rw}} \geq 0 \tag{39}$$

and

$$(F^p)'' = \frac{-\mu}{(K^p_{rw})^2} \left\{ K^p_{rw}(K^p_{rnw})'' - 2\,(K^p_t)'(K^p_{rnw})' \right\} \tag{40}$$

Finally, derivatives at (S_h, S_h) are defined in a similar way to

$$\partial_S^- K^{id,u}_{rw}(S_{id}, S_{id}) = \lim_{\delta \to 0} \frac{K^{id,u}_{rw}(S_{id}, S_{id}) - K^{id,u}_{rw}(S_{id} - \delta, S_{id})}{\delta} \tag{41}$$

$$\leq \lim_{\delta \to 0} \frac{K^i_{rw}(S_{id}) - K^i_{rw}(S_{id} - \delta)}{\delta} = \partial_S K^i_{rw}(S_{id}). \tag{42}$$

References

1. J. O. Amaefule and L. L. Handy. The effect of interfacial tension on relative oil/water permabilities of consolidated porous media. *Soc. Pet. Engrs. J.*, pages 371–381, June 1982.
2. S. E. Buckley and M. C. Leverett. Mechanisms of fluid displacement in sands. *Trans. Amer. Inst. Min. Meta. Engrs.*, 146:107–116, 1942.
3. Francis M. Carlson. Simulation of relative permeability hysteresis to the nonwetting phase. Paper SPE 10157 presented at the 56th Annual Fall Technical Conference and Exhibition of the Society of Petroleum Engineers of AIME, San Antonio, TX, Oct 5–7 1981.
4. J. Çolonna, F. Brissaud, and J. L. Millet. Evolution of capillarity and relative permeability hysteresis. *SPEJ Trans.*, 253:28–38, February 1972.
5. Forrest F. Craig. *The Reservoir Engineering Aspects of Waterflooding.* Monograph Series, Society of Petroleum Engineers, Dallas, 1971.
6. Attila I. Evrenos and A. G. Comer. Numerical simulation of hysteretic flow in porous media. Paper SPE 2693 prepared for the 44th Annual Fall Meeting of SPE of AIME, Denver, Co, Sept 28 -Oct 1 1969.
7. Khaled M. Furati. The solution of the Riemann problem for a hyperbolic system modeling polymer flooding with hysteresis. *J. Math. Anal. Appl.* To appear.
8. T. M. Geffen, W. W. Owens, D. R. Parrish, and R. A. Morse. Experimental investigation of factors affecting laboratory relative permeability measurements. *Trans. AIME*, 192:99–110, 1951.

9. Robert E. Gladfelter and Surendra P. Gupta. Effect of fractional flow hysteresis on recovery of tertiary oil. *Soc. Pet. Engrs. J.*, 20:508–520, December 1980.

10. Eli L. Isaacson. Global solution of a Riemann problem for a non-strictly hyperbolic system of conservation laws arising in enhanced oil recovery. Unpublished.

11. Thormod Johansen and Ragnar Winther. The solution of the Riemann problem for a hyperbolic system of conservation laws modeling polymer flooding. *SIAM J. Math. Anal.*, 19(3):541–566, May 1988.

12. S. C. Jones and W. O. Roszell. Graphical techniques for determining relative permeability from displacement experiments. *J. Pet. Tech.*, pages 807–816, May 1978.

13. J. E. Killough. Reservoir simulation with history-dependent saturation functions. *Soc. Pet. Engrs. J.*, 16:37–48, February 1976.

14. Carlon S. Land. Calculation of imbibition relative permeability for two– and three-phase flow from rock properties. *Soc. Pet. Engrs. J.*, pages 149–156, June 1968.

15. Carlon S. Land. The optimum gas saturation for maximum oil recovery from displacement by water. Paper SPE 2216 prepared for the 43rd Annual Fall Meeting of SPE of AIME, Houston, TX, Sept 29 -Oct 2 1968.

16. Carlon S. Land. Comparison of calculated with experimental imbibition relative permeability. *Soc. Pet. Engrs. J.*, pages 419–425, December 1971.

17. R. J. Lenhard and J. C. Parker. A model for hysteretic constitutive relations governing multiphase flow, 2. permeability-saturation relations. *Water Resources Res.*, 23(12):2197–2206, December 1987.

18. D. Marchesin, H. B. Medeiros, and P. J. Paes-Leme. A model for two phase flow with hysteresis. *Contemporary Math.*, 60:89–107, 1987.

19. J. Naar and J. H. Henderson. An imbibition model — its application to flow behavior and the prediction of oil recovery. *Soc. Pet. Engrs. J.*, 222:61–70, June 1961.

20. J. Naar and R. J. Wygal. Three-phase imbibition relative permeability. *Soc. Pet. Engrs. J.*, pages 254–258, December 1961.

21. J. Naar, R. J. Wygal, and J. H. Henderson. Imbibition relative permeability in unconsolidated porous media. *Soc. Pet. Engrs. J.*, 225:13–17, March 1962.

22. O. A. Oleinik. Uniqueness and a stability of the generalized solution of the Cauchy problem for a quasilinear equation. *Uspekhi Mat. Nauk*, 14:165–170, 1959. English translation in Amer. Math. Soc. Transl. Ser. 2, 33(1964), 285–290.

23. J. S. Osoba, J. G. Richardson, J. K. Kerver, J. A. Hafford, and P. M. Blair. Laboratory measurements of relative permeability. *Trans. AIME*, 192:47–56, 1951.

24. Gary A. Pope. The application of fractional flow theory to enhanced oil recovery. *Soc. Pet. Engrs. J.*, 20:191–205, 1980.

25. Pietro Raimondi and Michael A. Torcaso. Distribution of the oil phase obtained upon imbibition of water. *Soc. Pet. Engrs. J.*, pages 49–55, March 1964.

26. C. R. Sandberg, L. S. Gournay, and R. F. Sippel. The effect of fluid-flow rate and viscosity on laboratory determinations of oil-water relative permeabilities. *Trans. AIME*, 213:36–43, 1958.

27. R. W. Snell. Three-phase relative permeability in an unconsolidated sand. *J. Inst. Pet.*, 48(459):80–88, March 1962.

28. H. J. Welge. A simplified method for computing oil recovery by gas or water drive. *Trans. Amer. Inst. Min. Meta. Engrs.*, 195:91–98, 1952.

29. M. R. J. Wyllie and G. H. F. Gardner. The generalized Kozeny-Carman equation: Part 1 – review of existing theories. *World Oil*, 146:121–127, March 1958.

30. M. R. J. Wyllie and G. H. F. Gardner. The generalized Kozeny-Carman equation: Part 2 – a novel approach to problems of fluid flow. *World Oil*, 146:210–227, April 1958.